RESEARCH ARTICLE

Taste receptor type 1 member 3 enables western diet-induced anxiety in mice

Jae Won Song[1], Keon-Hee Lee[1], Hobin Seong[1], Dong-Mi Shin[1,2*] and Woo-Jeong Shon[1,2*]

Abstract

Background Accumulating evidence supports that the Western diet (WD), a diet high in saturated fat and sugary drinks, contributes to the pathogenesis of anxiety disorders, which are the most prevalent mental disorders worldwide. However, the underlying mechanisms by which WD causes anxiety remain unclear. Abundant expression of taste receptor type 1 member 3 (TAS1R3) has been identified in the hypothalamus, a key brain area involved in sensing peripheral nutritional signals and regulating anxiety. Thus, we investigated the influence of excessive WD intake on anxiety and mechanisms by which WD intake affects anxiety development using wild-type (WT) and *Tas1r3* deficient (*Tas1r3*$^{-/-}$) mice fed a normal diet (ND) or WD for 12 weeks.

Results WD increased anxiety in male WT mice, whereas male *Tas1r3*$^{-/-}$ mice were protected from WD-induced anxiety, as assessed by open field (OF), elevated plus maze (EPM), light–dark box (LDB), and novelty-suppressed feeding (NSF) tests. Analyzing the hypothalamic transcriptome of WD-fed WT and *Tas1r3*$^{-/-}$ mice, we found 1,432 genes significantly up- or down-regulated as a result of *Tas1r3* deficiency. Furthermore, bioinformatic analysis revealed that the CREB/BDNF signaling-mediated maintenance of neuronal regeneration, which can prevent anxiety development, was enhanced in WD-fed *Tas1r3*$^{-/-}$ mice compared with WD-fed WT mice. Additionally, in vitro studies further confirmed that *Tas1r3* knockdown prevents the suppression of *Creb1* and of CREB-mediated BDNF expression caused by high levels of glucose, fructose, and palmitic acid in hypothalamic neuronal cells.

Conclusions Our results imply that TAS1R3 may play a key role in WD-induced alterations in hypothalamic functions, and that inhibition of TAS1R3 overactivation in the hypothalamus could offer therapeutic targets to alleviate the effects of WD on anxiety.

Keywords Anxiety disorders, Western diet, Taste receptor type 1 member 3, Hypothalamus

Background

Anxiety disorders are defined as persistent, uncontrollable, and disproportionate feelings of anxiety that interfere with normal functioning in daily life [1]. Anxiety disorders have the highest prevalence of any mental disorder worldwide and are the leading cause of global disease burden (ranked as the eighth leading cause of years lived with disability in 2019) [2, 3]. Anxiety disorders are multifactorial mental illnesses that are influenced by genetic and environmental factors, such as childhood experiences, socioeconomic status, smoking, and alcohol abuse [4–6]. Among external factors, diet, one of the key factors that affects people's health in their daily lives, also affects anxiety [7]. Particularly, there is growing recognition that the Western diet (WD), which is rapidly increasing in consumption globally, can exacerbate anxiety [8, 9].

*Correspondence:
Dong-Mi Shin
shindm@snu.ac.kr
Woo-Jeong Shon
wjson@snu.ac.kr
[1] Department of Food and Nutrition, Seoul National University College of Human Ecology, Gwanak-Gu, Seoul 08826, Republic of Korea
[2] Research Institute of Human Ecology, Seoul National University, Gwanak-Gu, Seoul 08826, Republic of Korea

Song *et al. BMC Biology*   (2023) 21:243

Page 2 of 14

Several rodent and human studies suggest that neither diets high in sugar, nor fat-induced anxiety, always correlate with weight gain, nor does anxiety improve with weight loss [10, 11]. There are several limitations associated with lifestyle and weight control to relieve diet-induced mental disorders. There is also a lack of effective medications for anxiety, and the precise molecular mechanisms underlying WD-linked anxiety remain largely undetermined; further research is necessary.

The amygdala, hippocampus, medial prefrontal cortex, and hypothalamus form a network of brain structures involved in the neuropathophysiology of anxiety [12]. Among these brain regions, the hypothalamus is located close to the median eminence; this is composed of fenestrated capillaries so it can directly sense blood-borne molecules (e.g., nutrients and hormones) to regulate body homeostasis [13, 14]. This suggests that the hypothalamus is the primary site involved in the integration of peripheral nutritional signals and emotional responses. Studies of the pathogenesis of diet-induced anxiety as related to the principal features of the hypothalamus have focused on increased inflammation and hormonal dysregulation [15, 16]. However, hypothalamic neurogenesis modulated by diet has recently emerged as a new mechanism underlying diet-induced anxiety that affects the differentiation of anxiolytic neurons and hippocampal functions [17, 18].

Taste receptor type 1 member 3 (TAS1R3) is a G protein-coupled receptor (GPCR) involved in taste perception via the taste buds on the tongue [19]. TAS1R3 forms heterodimeric GPCR complexes such as TAS1R1/TAS1R3 (umami stimuli) and TAS1R2/TAS1R3 (sweet stimuli) to sense ligands [20]. TAS1R3 is reportedly expressed in various extraoral tissues, such as the epithelium of the gastrointestinal tract, pancreatic islet cells, and testes [21–23]. Furthermore, TAS1R3 signals are expressed more in neurons than in other brain cell types, with the highest expression in the hypothalamic paraventricular and arcuate nuclei compared to other brain regions, such as the cortex and hippocampus [24]. TAS1R3 is expressed in the hypothalamic regions, which are known to be involved in neuroendocrine control and hypothalamic neurogenesis, primarily mediating physiological and behavioral responses to nutrient fluxes in circulation [25, 26]. Although recent studies have shown that nutrient-sensing receptors expressed in the hypothalamus modulate diet-induced mood disorders, the role of TAS1R3 in WD-induced anxiety remains unknown [27, 28].

In this context, we hypothesized that nutrient-induced modulation of hypothalamic TAS1R3 is central to the regulation of WD-induced anxiety. To elucidate possible role of TAS1R3 in regulating behavior, we investigated *Tas1r3* deficient animals. We evaluated the influence of excessive WD intake on anxiety-related behavior and investigated the mechanisms through which WD intake affects anxiety development. Our findings uncover the previously unknown role of TAS1R3 in the context of WD-induced anxiety-like phenotype and may contribute to the development of preventive or therapeutic strategies for anxiety disorders.

Results

Male *Tas1r3*^{-/-} mice were protected against immobility and anxiety-like behavior induced by WD

To investigate the function of TAS1R3 in the behavioral performance of WD-fed mice, 8-week-old C57BL/6 WT and *Tas1r3*^{-/-} mice were fed an ND (10% fat diet with plain water) or WD (60% fat diet with 30% sucrose solution) for 12 weeks and subjected to a battery of behavioral tests. There was no significant difference between caloric intake between WT and *Tas1r3*^{-/-} mice (see Additional file 1: Fig. S1A-C). *Tas1r3* expression in the hypothalamus of WT mice was significantly increased by long-term WD intake (Fig. 1A). We first conducted an OF test (Fig. 1B) to assess the exploratory locomotor activity of mice exposed to the novel open field. WD-fed male WT mice showed relatively less travel in the arena and lower average velocity than ND-fed male WT mice and WD-fed male *Tas1r3*^{-/-} mice (Fig. 1C-D). Furthermore, the immobility time of male WT mice was significantly increased by WD, whereas WD-fed male *Tas1r3*^{-/-} mice had a similar range of locomotor activity to ND-fed male WT mice (Fig. 1E).

Regarding anxiety-related behavioral dimensions, WD-fed male WT mice were less inclined to encounter and travel the center zone than were ND-fed male WT mice, which is indicative of increased anxiety-like behavior. However, WD-fed male *Tas1r3*^{-/-} mice didn't exhibit WD-induced anxiety-behaviors (Fig. 1F-H). The EPM test was used to measure additional anxiety-like behaviors (Fig. 2A). We found that WD-fed male WT mice displayed increased anxiety-like behavior, as evident by fewer distance traveled in the open arms and less time spent in the open arms compared with ND-fed male WT mice. Contrastingly, WD-fed male *Tas1r3*^{-/-} mice showed more time spent in the open arms compared with WD-fed male WT mice (Fig. 2D). In addition, WD-fed male WT mice were more likely to spend time in the closed arms than both ND-fed male WT and WD-fed male *Tas1r3*^{-/-} mice (Fig. 2E). In the LDB test, WD-fed male WT mice spent significantly less time in the light zone compared to ND-fed male WT mice, whereas WD-fed male *Tas1r3*^{-/-} mice spent more time in the light zone than WD-fed male WT mice (Fig. 2F-H). In line with the results of the OF,
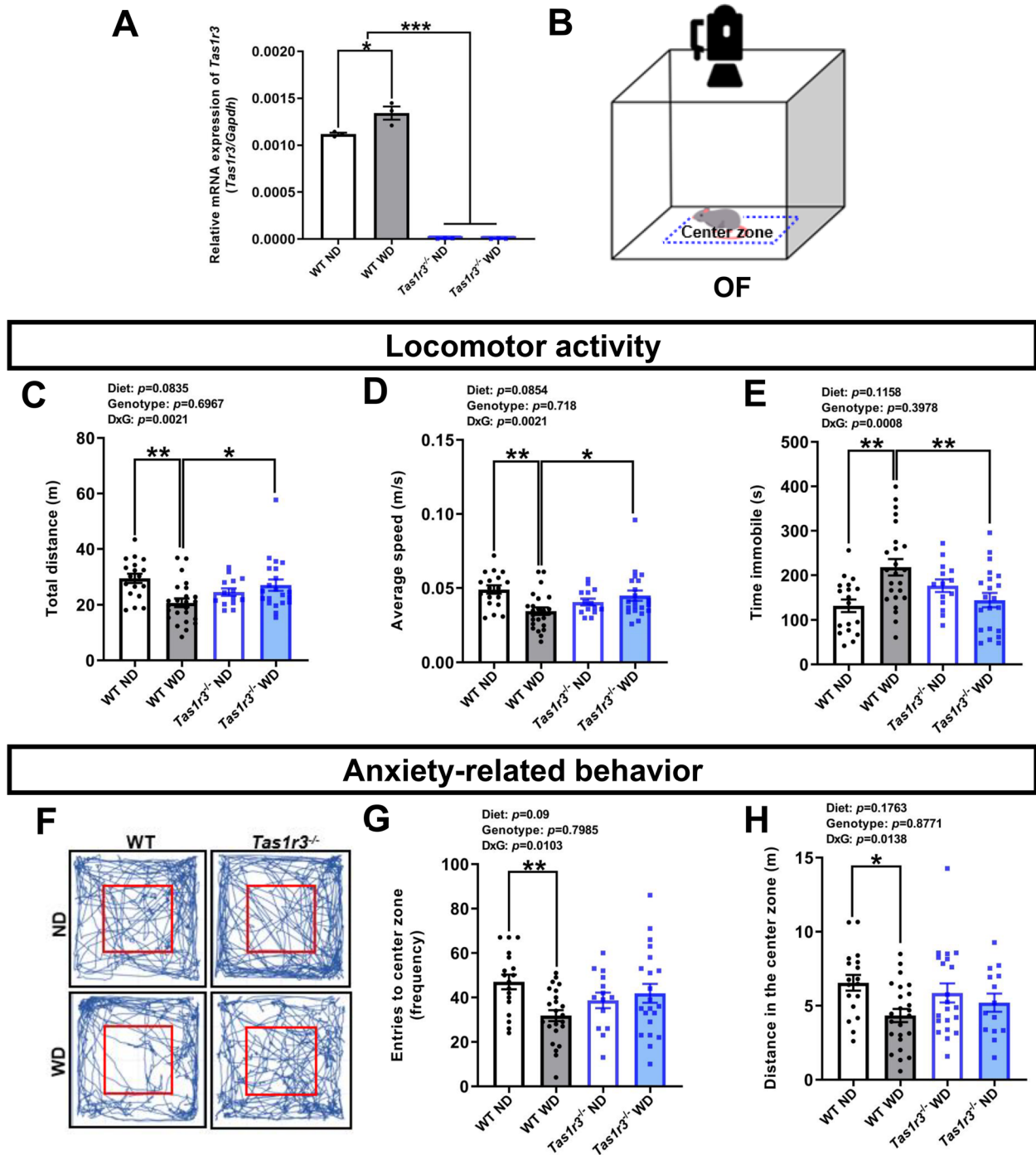
Fig. 1 WD-induced immobility and anxiety-related behaviors in WT mice not exhibited in WD-fed *Tas1r3⁻/⁻* mice. **A** *Tas1r3* mRNA expression in the hypothalamus of all groups. Two-way ANOVA followed by Tukey's multiple comparison test: *$p < 0.05$, ***$p < 0.001$. $n = 3$ mice/group. **B** Schematic diagram of the OF test. The inner blue dotted line denotes the center zone. **C-E** Locomotor activities assessed by total distance traveled in the arena, average speed and time spent immobile. Two-way ANOVA followed by Tukey's multiple comparison test: *$p < 0.05$, **$p < 0.01$. **F** Representative movement traces (blue lines) in OF chamber. **G,H** Anxiety-related behaviors measured by the frequency of entries to the center zone, and distance traveled in the center zone. Two-way ANOVA followed by Tukey's multiple comparison test: *$p < 0.05$, **$p < 0.01$. WT ND: $n = 18$; WT WD: $n = 24$; *Tas1r3⁻/⁻* ND: $n = 14$; *Tas1r3⁻/⁻* WD: $n = 21$. All values are presented as the means ± SEM. ANOVA, analysis of variance; OF, open field; ND, normal diet; WD, western diet; WT, wild-type

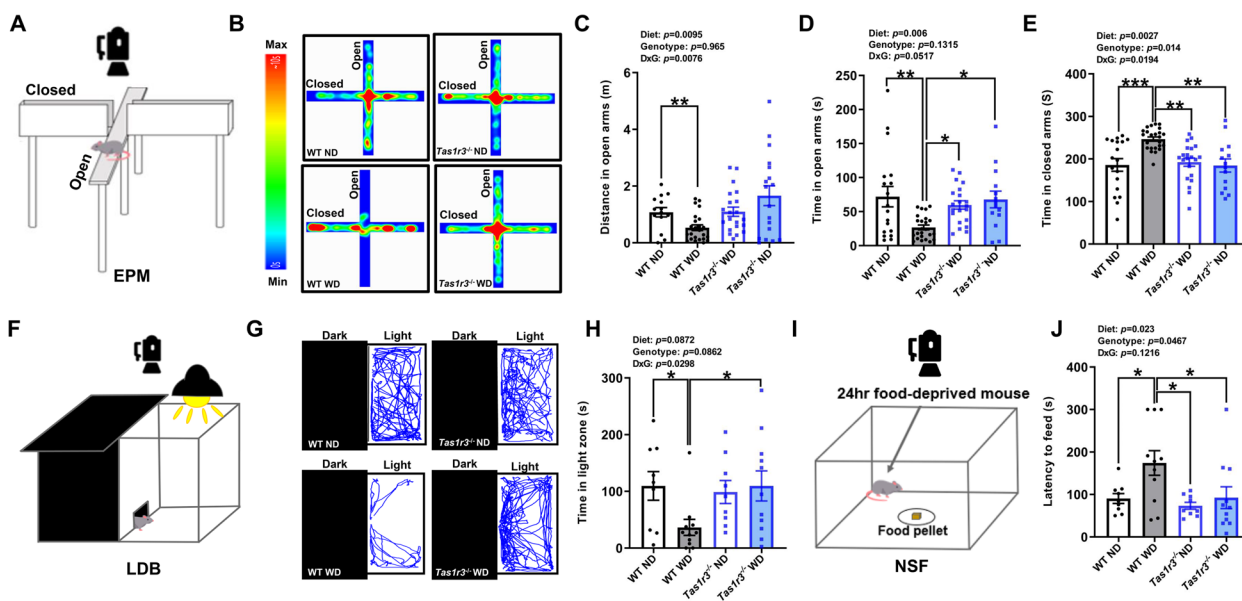Song *et al. BMC Biology*   (2023) 21:243

Page 4 of 14

Fig. 2 *Tas1r3* deficiency protects against the anxiety-like phenotypes induced by WD. **A** Schematic of EPM test. **B** Representative heatmaps of time spent in EPM. **C** Distance traveled in the open arms. Two-way ANOVA followed by Tukey's multiple comparison test: **$p < 0.01$. **D** Time spent in open arms. Two-way ANOVA followed by Tukey's multiple comparison test: *$p < 0.05$, **$p < 0.01$. **E** Time spent in closed arms. Two-way ANOVA followed by Tukey's multiple comparison test: **$p < 0.01$, ***$p < 0.001$. WT ND: $n = 18$; WT WD: $n = 24$; $Tas1r3^{-/-}$ ND: $n = 14$; $Tas1r3^{-/-}$ WD: $n = 21$. **F** Schematic of LDB test. **G** Representative movement traces (blue lines) in LDB. **H** Time spent in light zone. Two-way ANOVA followed by Tukey's multiple comparison test: *$p < 0.05$. WT ND: $n = 9$; WT WD: $n = 11$; $Tas1r3^{-/-}$ ND: $n = 9$; $Tas1r3^{-/-}$ WD: $n = 11$. **I** Schematic of NSF test. **J** Latency time to feed. Two-way ANOVA followed by Tukey's multiple comparison test: *$p < 0.05$. WT ND: $n = 9$; WT WD: $n = 11$; $Tas1r3^{-/-}$ ND: $n = 9$; $Tas1r3^{-/-}$ WD: $n = 11$. All values are presented as the means ± SEM. ANOVA, analysis of variance; EPM, elevated plus maze; LDB, Light–dark box; ND, normal diet; NSF, novelty-suppressed feeding; WD, western diet; WT, wild-type

EPM, and LDB tests, WD-fed male WT mice exhibited longer latency time for eating pellets compared with ND-fed male WT mice and WD-fed male $Tas1r3^{-/-}$ mice in NSF test (Fig. 2I-J).

After 12 weeks of high-calorie western diet intake, significant differences in body weight were observed between groups in male mice (see Additional file 1: Fig. S2A). Several studies showed that high-calorie western diet-induced obesity is a potential risk factor for anxiety [29, 30]. Therefore, we investigated whether WD-induced anxiety is dependent on weight gain. Linear regression analysis based on groups confirmed no significant association between body weights and anxiety-related parameters (see Additional file 1: Fig. S2B-H). To assess the effect of weight gain, we further analyzed the anxiety-related parameters using ANCOVA with body weights as the potential covariates. However, the ANCOVA model demonstrated that body weight was not a covariate significantly influencing anxiety-related behaviors (entries to center zone: $F = 0.065$, $p = 0.8$; distance in the center zone: $F = 0.003$, $p = 0.958$; distance in open arms: $F = 2.414$, $p = 0.125$; time in open arms: $F = 1.501$, $p = 0.225$; time in closed arms: $F = 2.71$, $p = 0.104$; time in light zone: $F = 1.613$, $p = 0.212$; latency to feed: $F = 1.083$, p

$= 0.305$). These results suggest that the anxiety levels of male mice were independent of their body weights.

There were significant differences in body weight between groups in female mice, similar to the phenotype we observed in male mice (see Additional file 1: Fig. S3A). However, there was no significant difference in locomotor activities and anxiety-related behaviors between groups in female mice (see Additional file 2: Fig. S3B-E), likely due to reported sex-dependent effects in anxiety-related behaviors [31].

These results suggest that consumption of WD can lead to increased anxiety in WT mice. However, $Tas1r3^{-/-}$ mice were protected from the WD-induced anxiety.

Tas1r3 deficiency largely alters gene expression in the hypothalamus of WD-fed mice

Considering that the anxiety levels of WD-fed male WT and $Tas1r3^{-/-}$ mice were not explained by their body weight, we investigated the underlying molecular mechanisms in the hypothalamus, a brain structure primarily involved in anxiety. We used RNA sequencing to identify the gene expression profile in the hypothalamus of WD-fed WT mice versus WD-fed $Tas1r3^{-/-}$ mice. Principal component analysis revealed that the hypothalamic transcriptome profiles of WD-fed $Tas1r3^{-/-}$ mice were distinct

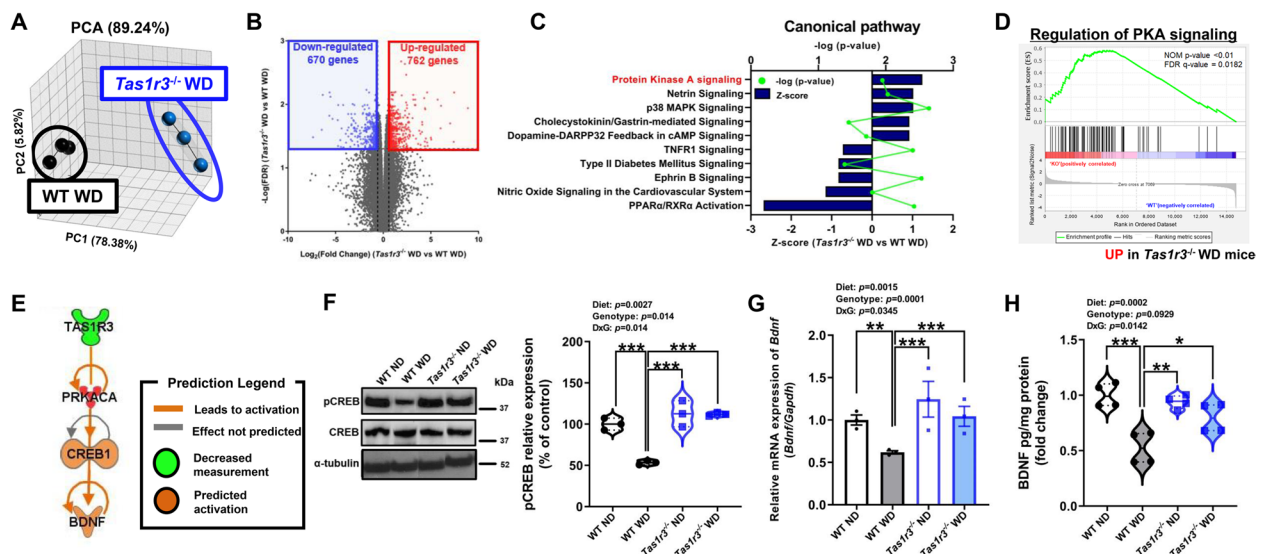Song *et al. BMC Biology*   (2023) 21:243

Page 5 of 14

Fig. 3 *Tas1r3* deficiency largely alters gene expression in the hypothalamus of WD-fed mice. **A** 3-D view of principal component analysis of the WD-fed *Tas1r3*$^{-/-}$ group versus the WD-fed WT group. Groups are represented by different colors, and dots show individual strains. Black spots represent the WT WD group and blue spots represent the *Tas1r3*$^{-/-}$ WD group. $n = 3$ mice/group. **B** Volcano plot of all DEGs between the WT WD group and the *Tas1r3*$^{-/-}$ WD group. Red dots indicate high relative expression of genes ($n = 762$), and blue dots indicate low relative expression of genes ($n = 670$). Unpaired two-tailed Student t-test: Thresholds of FDR < 0.05 and 1.5-fold change restriction analysis. **C** Canonical pathway significantly detected in WD-fed *Tas1r3*$^{-/-}$ mice compared to WD-fed WT mice: Right-tailed Fisher's exact test in IPA. Dots represent −log(p-value) and bars represent Z-score. **D** GSEA related to PKA signaling; genes were ordered by expression fold-changes upon *Tas1r3* deficiency in descending order from left to right. DEGs belonging to the enriched hallmark gene sets identified by GSEA. **E** Transcriptional regulator predicted to regulate DEGs. **F** (Left) Western blot analysis of phosphorylated CREB protein and CREB protein levels in hypothalamus of WT and *Tas1r3*$^{-/-}$ mice fed ND or WD for 12 weeks. (Right) Quantification of the total phosphorylated CREB protein levels in hypothalamus of mice. Two-way ANOVA followed by Tukey's multiple comparison test: ***$p < 0.001$. $n = 3$ mice/group. **G** qPCR validation of *Bdnf* mRNA expression. Two-way ANOVA followed by Tukey's multiple comparison test: **$p < 0.01$, ***$p < 0.001$. $n = 3$ mice/group. **H** BDNF protein levels in hypothalamus lysates from WT and *Tas1r3*$^{-/-}$ mice ND or WD for 12 weeks. Two-way ANOVA followed by Tukey's multiple comparison test: *$p < 0.05$, **$p < 0.01$, ***$p < 0.001$. $n = 4$ mice/group. All values are presented as mean ± SEM. ANOVA, analysis of variance; BDNF, brain-derived neurotrophic factor; CREB, cAMP response element-binding protein; DEGs, differentially expressed genes; FDR, false discovery rate; GSEA, gene set enrichment analysis; IPA, ingenuity pathway analysis; ND, normal diet; PKA, protein kinas A; WD, western diet; WT, wild-type

from those of WD-fed WT mice (Fig. 3A). We found that 1,432 genes were expressed significantly differently, with 762 upregulated genes and 670 downregulated genes (with a fold change greater than 1.5 or less than -1.5, and a false discovery rate (FDR) <0.05, which were selected as baseline differentially expressed genes (DEGs) in WD-fed *Tas1r3*$^{-/-}$ mice compared to WD-fed WT mice (Fig. 3B).

Next, we investigated the implicit mechanism of WD-induced anxiety prevented by *Tas1r3* deficiency by confirming the top significant canonical pathways by IPA (ingenuity pathway analysis). Protein kinase A (PKA) signaling was the most activated pathway in WD-fed *Tas1r3*$^{-/-}$ mice compared to WD-fed WT mice ($p = 0.01122$; Fig. 3C). Furthermore, gene set enrichment analysis (GSEA) showed that the regulation of PKA signaling was significantly upregulated in WD-fed *Tas1r3*$^{-/-}$ mice compared to WD-fed WT mice (nominal p value < 0.01; Fig. 3D).

IPA predicted the activation of CREB (cAMP response element-binding protein) (Fig. 3E), a key downstream target of the PKA signaling cascade, and we confirmed that the phosphorylated CREB protein level was significantly lower in WD-fed WT mice than both ND-fed WT mice and WD-fed *Tas1r3*$^{-/-}$ mice (Fig. 3F). In addition, WD intake decreased *Bdnf* mRNA expression level in WT mice, whereas WD-fed *Tas1r3*$^{-/-}$ mice didn't show decreased *Bdnf* expression (Fig. 3G). To validate whether differences in the transcript levels of BDNF regulated by *Tas1r3* deficiency, an enzyme-linked immunosorbent assay (ELISA) was conducted. Consistently, the level of hypothalamic BDNF protein was also decreased by WD in WT mice, but not in WD-fed *Tas1r3*$^{-/-}$ mice (Fig. 3H).

CREB and CREB-mediated downstream molecules have been reported to enhance neurogenesis and suppress neuronal cell death [32]. Thus, these results highlight that *Tas1r3* deficiency alters CREB/BDNF
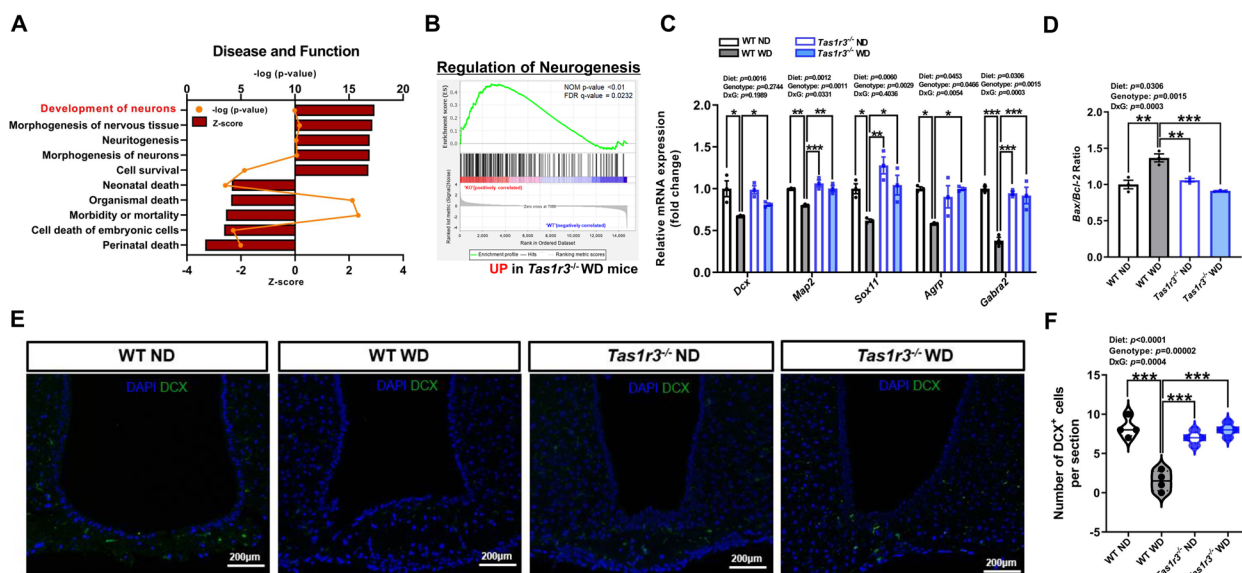
Song *et al. BMC Biology*   (2023) 21:243

Page 6 of 14

Fig. 4 WD-fed *Tas1r3*$^{-/-}$ mice displayed maintained hypothalamic neurogenesis compared to WD-fed WT mice. **A** Significantly detected disease and function in WD-fed *Tas1r3*$^{-/-}$ mice compared to WD-fed WT mice. Right-tailed Fisher's exact test in IPA. Dots represent –log(p-value) and bars represent Z-score for each disease and function annotated. **B** GSEA related to neurogenesis. **C** qPCR validation of mRNA expression of neuronal progenitor cell markers and hypothalamus-related neuronal cell markers of the hypothalamus. Two-way ANOVA followed by Tukey's multiple comparison test: $*p < 0.05$, $**p < 0.01$, and $***p < 0.001$. $n = 3$ mice/group. **D** qPCR validation of *Bax* to *Bcl-2* mRNA expression ratio. Two-way ANOVA followed by Tukey's multiple comparison test: $**p < 0.01$, $***p < 0.001$. $n = 3$ mice/group. **E** DCX staining of regions of the hypothalamus in each group. **F** The number of DCX-positive cells per field in regions of the hypothalamus. Two-way ANOVA followed by Tukey's multiple comparison test: $***p < 0.001$. $n = 2$ slices from 2 mice/group. All data are presented as mean ± SEM. ANOVA, analysis of variance; GSEA, gene set enrichment analysis; IPA, ingenuity pathway analysis; ND, normal diet; WD, western diet; WT, wild-type

signaling in the hypothalamus of WD-fed mice, thereby preventing the pathogenesis of WD-induced anxiety.

Hypothalamic neurogenesis was maintained in WD-fed *Tas1r3*$^{-/-}$ mice compared with WD-fed WT mice

To identify the functional annotation of DEGs affected by *Tas1r3*, we categorized these genes based on their relevance to disease and biological functions and tested their Z-scores using IPA. Disease and function analysis revealed that the most increased functions in WD-fed *Tas1r3*$^{-/-}$ mice compared to WD-fed WT mice included the development of neurons ($p = 1.06E-10$), morphogenesis of nervous tissue ($p = 3.8E-11$), and neuritogenesis ($p = 7.65E-11$), whereas the most decreased functions were perinatal death ($p = 1.07E-05$), cell death of embryonic cells ($p = 5.21E-05$), morbidity or mortality ($p = 1.43E-16$) in WD-fed *Tas1r3*$^{-/-}$ mice compared to WD-fed WT mice (Fig. 4A). Furthermore, GSEA confirmed that neurogenesis was significantly upregulated in WD-fed *Tas1r3*$^{-/-}$ mice compared with WD-fed WT mice (nominal *p* value < 0.01; Fig. 4B).

Expectedly, qPCR validation revealed that the transcript levels of *Dcx*, the neuroblast marker, and *Map2*, the mature neuron marker, were markedly decreased in WD-fed WT mice compared to that in ND-fed WT

mice. Furthermore, *Agrp* expressed in functional neurons differentiated from hypothalamic neuronal precursor cells and *Gabra2*, a GABAergic neuron marker, were found to be significantly lower than both ND-fed WT mice and WD-fed *Tas1r3*$^{-/-}$ mice (Fig. 4C). In addition, the ratio of *Bax* to *Bcl2*, a marker of cell susceptibility to apoptosis, was significantly increased in WD-fed WT mice relative to ND-fed WT mice whereas it remained significantly decreased in WD-fed *Tas1r3*$^{-/-}$ mice (Fig. 4D).

Nissl bodies are discrete granular structures in neurons that are generally stained to visualize the neurons in the brain. To investigate the quantity of intact neurons in the hypothalamus of mice fed WD, Nissl staining was conducted, and the percentage of intact neurons in selected areas was measured using ImageJ software. We observed a marked decrease in the percentage of intact neuronal cells in hypothalamus sections from WD-fed WT mice compared to both ND-fed WT mice and WD-fed *Tas1r3*$^{-/-}$ mice (see Additional file 1: Fig. S3A-B). Furthermore, the number of DCX-immunopositive cells in WD-fed *Tas1r3*$^{-/-}$ mice was similar to that in ND-fed WT, whereas it decreased in WD-fed WT mice compared to that in ND-fed WT mice (Fig. 4E-F).

Song *et al. BMC Biology*   (2023) 21:243

Page 7 of 14

These results suggest that *Tas1r3* deficiency alleviates the WD-induced suppression of neurogenesis in the hypothalamus.

Tas1r3 knockdown prevented WD-induced suppression of CREB/BDNF signaling in the adult hypothalamic neuronal cell line

Since we used conventional knockout mice, we investigated whether *Tas1r3* directly modulated CREB/BDNF signaling in hypothalamic neurons. We transfected the hypothalamic neuronal cell line, mHypoA-2/12 cells
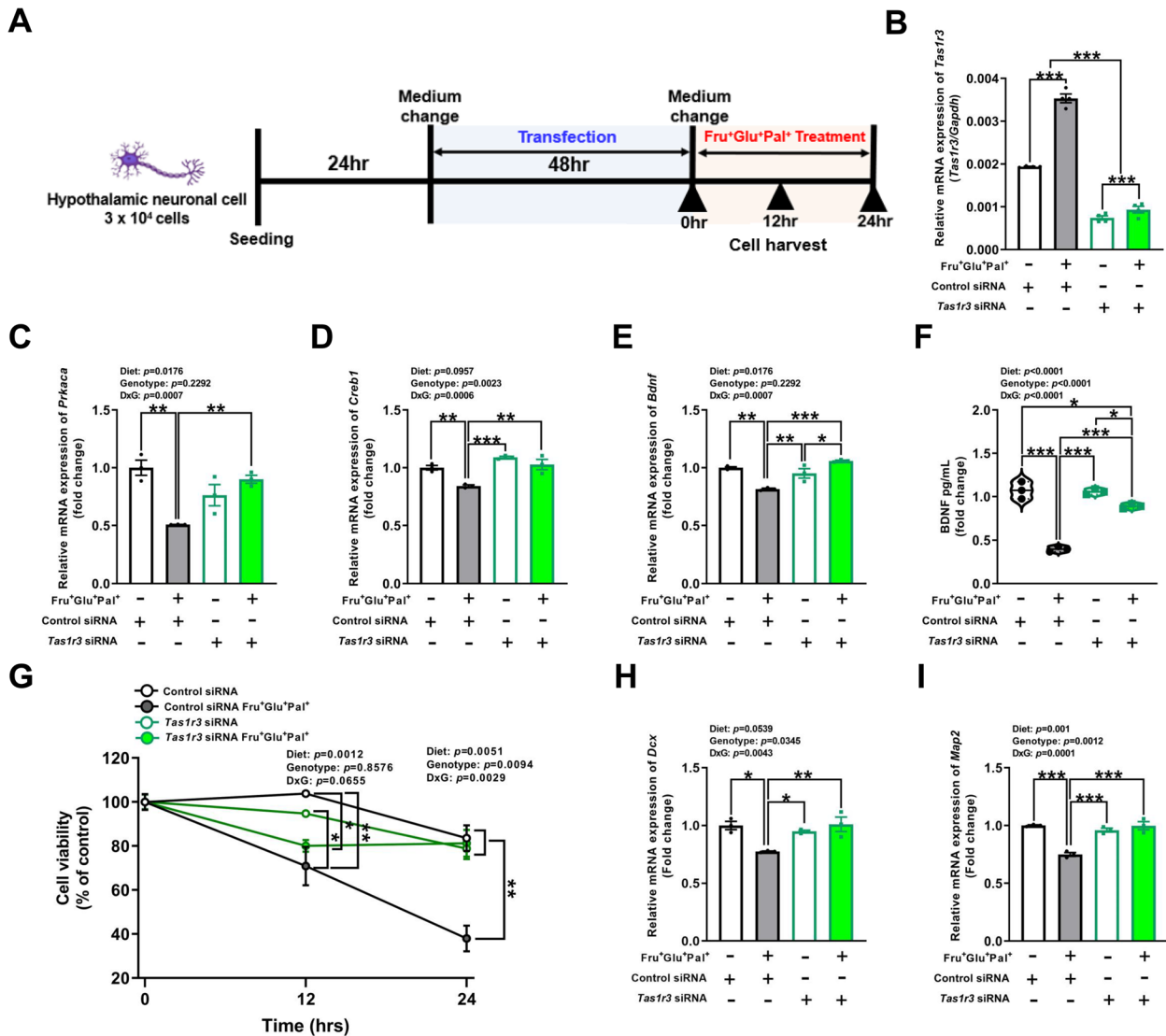

Fig. 5 *Tas1r3* knockdown alleviates high glucose, fructose and palmitate-induced suppression of CREB/BDNF signaling in hypothalamic neuronal cell. **A** Study design of siRNA knockdown in hypothalamic neuronal cell line mHypoA-2/12. **B** Evaluation of siRNA-mediated *Tas1r3* mRNA suppression in a cultured adult hypothalamic neuronal cell line after 48 h of transfection. Two-way ANOVA followed by Tukey's multiple comparison test: ***p < 0.001. *n* = 4/group. **C-E** mHypoA-2/12 cells were transfected with *Tas1r3* siRNA or scrambled control siRNA for 48 h and stimulated with or without fructose (10 mM), glucose (10 mM), and palmitate (10 μM) for 24 h. Relative mRNA expression of *Prkaca*, *Creb1*, and *Bdnf*. Two-way ANOVA followed by Tukey's multiple comparison test: *p < 0.05, **p < 0.01, and ***p < 0.001. *n* = 3/group. **F** Protein levels of BDNF released into the supernatant. Two-way ANOVA followed by Tukey's multiple comparison test: **p < 0.01, ***p < 0.001. *n* = 3/group. **G** mHypoA-2/12 cell viability at 0, 12, and 24 h. Two-way ANOVA followed by Tukey's multiple comparison test: *p < 0.05, **p < 0.01. *n* = 3/group. **H,I** Relative mRNA expression of *Map2* and *Dcx*. Two-way ANOVA followed by Tukey's multiple comparison test: *p < 0.05, **p < 0.01, and ***p < 0.001. *n* = 3/group. All data are presented as mean ± SEM. ANOVA, analysis of variance; BDNF, brain-derived neurotrophic factor; CREB, cAMP response element-binding protein

with siRNA targeting *Tas1r3* and treated the cell culture media containing 10mM fructose, 10mM glucose, and 10µM palmitate (a major component of dietary fat) to create WD conditions for the cell line (Fig. 5A). We found that *Tas1r3* mRNA expression was significantly suppressed by siRNA compared to the control. Furthermore, we confirmed that the WD condition significantly increased *Tas1r3* expression (Fig. 5B). The knockdown of *Tas1r3* significantly prevented the decrease in the mRNA expression of *Prkaca*, *Creb1,* and *Bdnf* induced by the WD condition (Fig. 5C-E). ELISA-based quantification of BDNF protein released into the supernatant validated the changes in the transcript levels of *Bdnf* by *Tas1r3* knockdown (Fig. 5F). Furthermore, cell viability calculated at 12 hr after ND- or WD-conditioned treatment, both groups conditioned with WD showed lower cell viability compared to controls. However, decrease in viability at 24 hr was not observed in the WD-conditioned *Tas1r3* siRNA group, whereas WD-conditioned control siRNA group showed significantly lower viability compared to both the control and WD-conditioned *Tas1r3* siRNA group (Fig. 5G). As expected, the *Tas1r3* knockdown ameliorated suppressed expression of *Dcx* and *Map2* by WD conditioned media (Fig. 5H-I).

Discussion

We demonstrated that prolonged WD consumption can exacerbate anxiety in male mice, independent of weight gain, as reported in previous studies [33–35]. Furthermore, TAS1R3 modulates CREB-mediated neuronal regeneration in WD-fed mice. Ultimately, we displayed that TAS1R3 is a key regulator of nutritional stimulus-induced anxiety by altering hypothalamic function.

Obesity, which is caused by long-term high-calorie consumption, can increase anxiety through insulin or leptin resistance, systemic inflammation, and hormonal dysregulation [36]. TAS1R3, which is expressed in metabolic tissues such as adipocytes and pancreatic β cells, has been reported to regulate metabolism [37, 38]. Studies on mice with genetic ablation of TAS1R3 revealed differences in weight gain compared to WT mice [39, 40]. Here, in our *in vivo* model, WD-fed *Tasr3*$^{-/-}$ mice also showed less weight gain compared to WD-fed WT mice. However, we confirmed that the anxiety levels of mice were independent of their body weights by linear regression analysis and ANCOVA. These results suggest that molecular mechanisms in the brain, not weight gain, may be involved in the alterations of anxiety-related phenotypes caused by *Tas1r3* deficiency.

Regarding TAS1R3 and brain functions, only behavioral dysfunction by hippocampal neurodegeneration in *Tas1r3* deficient mice fed a normal chow diet have previously been reported [41]. In contrast, in our model, in which *Tas1r3* deficient mice were fed WD for 12 weeks, *Tas1r3* deficiency-mediated neuroprotective effects in the hypothalamus of WD-fed mice reduced WD-induced immobility and anxiety-like behaviors, but there were no behavioral changes in ND-fed mice. Unlike the hypothalamus, the WD condition did not alter *Tas1r3* mRNA expression levels in the hippocampus and hippocampal neuronal cell line (see Additional file 1: Fig.S5A-B). Furthermore, there was no significant difference in *Prkaca*, *Creb1* and *Bdnf* mRNA expression in hippocampus and hippocampal neuronal cell line between groups (see Additional file 1: Fig. S5C-D). These results suggest that TAS1R3 may have different regulatory activities, depending on the brain region and nutritional status.

The molecular mechanisms by which TAS1R3 regulates anxiety remain unclear. Hence, we performed transcriptomic analysis of the hypothalamus of WD-fed WT and *Tas1r3*$^{-/-}$ mice. PKA signaling was identified as the main pathway that was increased in WD-fed *Tas1r3*$^{-/-}$ mice compared to WD-fed WT mice. The hypothalamus is characterized as the center of integration of peripheral nutrient-related signals, such as circulating adiposity hormones, gastric hormones, and nutrients [42]. Particularly, the median eminence of the hypothalamus is in contact with fenestrated capillaries, providing privileged access to nutritional signals carried by the blood stream [25]. Furthermore, the PKA signaling cascade in the hypothalamus can be reportedly activated by nutritional signals, such as fasting state, or suppressed by a hypercaloric diet by G-protein coupled receptor-mediated mechanisms signaling [27, 43], suggesting a potential mechanism by which interruption of nutrient sensing by TAS1R3 prevents WD-induced suppression of PKA.

In the brain, the interplay between the transcriptional controller CREB, a key downstream target of PKA, and neurotrophic ligands such as brain-derived neurotrophic factor (BDNF) is crucial for synaptic plasticity and neuronal development [44, 45]. Compared to WD-fed WT mice, the hypothalamus of WD-fed *Tas1r3*$^{-/-}$ mice showed significant increases in the phosphorylated CREB protein and CREB-mediated genes such as *Arc*, *Erg1*, *Vegfa,* and *Bdnf.* CREB is activated by multiple signaling pathways during synaptic strengthening, plasticity, and neurogenesis, which are related to brain function [46, 47]. Furthermore, BDNF levels were found to be lower in people with anxiety disorders [48] and hypothalamic gene transfer of BDNF reduced anxiety-like behaviors in rodents [49, 50]. BDNF can also induce hypothalamic neurogenesis, which can affect diverse functions of the hypothalamus [51].

Although hippocampal neurogenesis has received the most attention [52], evidence of hypothalamic neurogenesis and its importance in biological functions has

Song *et al. BMC Biology*   (2023) 21:243

Page 9 of 14

recently been reported [53]. Here, we found that neuronal development was the most activated biological function in WD-fed *Tas1r3*-/- mice compared to WT mice. Furthermore, chronic consumption of a high-calorie diet suppressed neuronal turnover in the arcuate nucleus by increasing apoptosis of newborn neurons [54]. We found that the ratio of *Bax* to *Bcl2* (a marker of cell susceptibility to apoptosis) [55], was significantly decreased in WD-fed *Tas1r3*-/- mice, suggesting that *Tas1r3* deficiency may increase resistance to WD-induced neuronal death. Anxiety is affected by hypothalamic neurogenesis by modulating the differentiation of anxiolytic neurons [56]. Neuronal stem cells in the hypothalamus differentiate into functional neurons that express the neuropeptides AgRP and POMC, which are involved in feeding regulation [57]. Interestingly, we confirmed that the mRNA expression level of *Agrp* was increased in WD-fed *Tas1r3*-/- mice compared to WD-fed WT mice. AgRP neurons have been reported to modulate fasting-induced anxiolytic effects [58], suggesting that decreased AgRP-expressing neurons in WD-fed WT mice might increase anxiety-like phenotypes. Moreover, *Gabra2*, a GABAergic neuron marker, was significantly increased in WD-fed *Tas1r3*-/- mice compared to WT mice. The GABA$_A$α2 subunit (the *Gabra2* gene) plays an important role in the regulation of anxiety being modulated by benzodiazepines, barbiturates, and ethanol [59, 60]. These results indicate that enhanced hypothalamic neurogenesis in WD-fed *Tas1r3*-/- mice compared to WD-fed WT mice may lead to the regeneration of anxiety-regulating neurons.

To the best of our knowledge, this is the first report to identify a key regulator of neuronal function in the hypothalamus during stress induced by diet, one of the key environmental factors in our lives. The findings from our rodent model confirmed that *Tas1r3* deficiency prevents WD-induced neuronal loss and anxiety. However, despite the genetic similarity, further human studies are needed to investigate the association between TAS1R3 expression levels and anxiety status in people consuming Western diets.

Conclusions

In summary, we demonstrated that *Tas1r3* deficiency maintains neuronal regeneration in the hypothalamus of male mice under dietary stimuli by activating CREB/BDNF signaling, which regulates neuronal plasticity and development. A key finding of our study is that nutrient molecules, rather than peripheral hormones, directly affect neuronal survival and renewal via the nutrient-sensing receptor, TAS1R3. Additionally, TAS1R3 is a GPCR, which is a major therapeutic target for approved drugs [61], suggesting that it could be a novel therapeutic target for diet-induced anxiety. The present study provides the first comprehensive description of the roles of TAS1R3 in the hypothalamus, providing additional evidence of causality between WD and anxiety and revealing the previously unexplained mechanism of WD-induced anxiety.

Methods

Mice and diets

WT C57BL/6 (RRID:IMSR_JAX 000664) and Tas1r3t-mCSZ (RRID:IMSR_JAX 013066) mice were purchased from Jackson Laboratory (Bar Harbor, ME, USA). Male heterozygous with female heterozygous mice were used to generate *Tas1r3*-/- and littermate WT mice. *Tas1r3*-/- mice were backcrossed with WT C57BL/6 mice for at least seven generations. *Tas1r3*-/- mice weighing 23–25 g and age- and weight-matched WT littermates were housed in a specific pathogen-free animal facility. A high-fat diet (D12492) and matched control diet (D12450J) were purchased from Research Diet Inc. (New Brunswick, NJ, USA). Male WT and *Tas1r3*-/- mice were randomly divided into four groups: (1) WT ND, WT mice received a control diet with plain water ; (2) *Tas1r3*-/- ND, *Tas1r3*-/- mice received a control diet with plain water; (3) WT WD, WT mice received a high-fat diet with 30% (w/v) sucrose solution; and (4) *Tas1r3*-/- WD, *Tas1r3*-/- mice received a high-fat diet with 30% (w/v) sucrose solution. Food and drinks were provided *ad libitum* for 12 weeks. Mice were group-housed with 2–3 mice per cage in the same room to minimize any environmental effects and maintained according to the guidelines of the Seoul National University Animal Experiment Ethics Committee. All experiments were approved by the Institutional Animal Care and Use Committee of Seoul National University (approval number: SNU-181001-2; Seoul, Korea).

Behavioral assessment

Two cohorts of animals were produced (Additional file 2: Table S1) to conduct behavioral testing. Behavioral tests were conducted to assess locomotor activities and anxiety-like behaviors as detailed below.

Open field test

Locomotor activity and anxiety-like behaviors of the mice were assessed using a rectangular chamber (W × L × D = 40 cm × 40 cm × 40 cm). The mice were acclimatized to the room for 1h before the test. The mice were then introduced into the chamber, and all mouse activities were recorded for 10 min. Activity-monitoring software (ANY-Maze, Stoelting Co., Wood Dale, IL, USA)

was used to calculate multiple parameters, such as total distance traveled, velocity, and mobility over the duration of the 10-min test. Freezing time in the central 25% of the chamber (center zone) and entries or line crossings to the center zone were measured to quantify anxiety. At the end of each test, the chamber was cleaned using 70% ethanol.

Elevated plus maze test

Anxiety-related behaviors were assessed using an EPM. The entire apparatus was 50 cm above the floor and consisted of two open arms (W × L = 5 cm × 30 cm) and two closed arms (W × L = 5 cm × 30 cm) attached to a central platform (W × L = 5 cm × 5 cm). Mice were placed on the center platform of the apparatus facing an open arm, and mouse movements were recorded for 5 min. ANY-Maze software (Stoelting Co., Wood Dale, IL, USA) was used to calculate the time spent in the arms, to quantify anxiety. The time spent in the closed or open arms was divided by the total time spent in the arms. At the end of each test, the apparatus was cleaned using 70% ethanol.

Light-Dark box test

Anxiety-related behaviors were assessed using the LDB test. The LDB test was conducted as described previously [41]. A dark chamber (W × L × D = 40 cm × 20 cm × 40 cm) was inserted to the rectangular chamber used in the open field test to perform this test. The LDB was divided into a dark (lux 1) and a light (lux 400) zone and interconnected by an entry (W × L = 7 cm × 7 cm) in the partition wall. Mice were placed on the center of the dark zone and mouse movements were recorded for 10 min. Anxiety was calculated based on the time spent in the light zone using ANY-Maze software (Stoelting Co., Wood Dale, IL, USA). At the end of each test, the chamber was cleaned using 70% ethanol.

Novelty-suppressed feeding test

To assess anxiety behavior, NSF test was conducted. Food was removed at 24 hr before testing, although water was available *ad libitum*. For testing, mice were placed in an open field (W × L × D = 50 cm × 50 cm × 20 cm) that contained a food pellet on a circular filter paper (10 cm in diameter) in the center of the apparatus. Mice were monitored for 5min and the latency to approach the food pellet was measured to quantify anxiety.

RNA isolation and gene expression profiling by RNA-seq

After 12 weeks of diet induction, all mice were anesthetized and euthanized by intraperitoneal injection of 20% urethane. Tissue samples from the hypothalamus stored at -80 °C were homogenized using TissueLyser II (QIACEN, Crawley, UK), and total RNA was extracted and purified using a DNA-free RNA isolation kit (RNAqueous-4PCR kit; Ambion, Austin, TX, USA), according to the manufacturer's instructions. Before RNA sequencing, the quality and concentration of extracted total RNA was confirmed using an Agilent 2100 Bioanalyzer (Agilent Technologies, Palo Alto, CA, USA). Out of the samples with an RNA integrity number greater than 8 were randomly selected for sequencing. $n = 3$ mice/group.

Bioinformatic analysis of Next-Generation RNA-seq

Raw RNA-seq reads were divided into individual samples based on their barcodes, and quality was controlled using the FASTQC tool as previously described [62]. The reads were analyzed using Partek Flow software (Parteck, St. Louis, MO, USA; http://www.partek.com/partekgs). Briefly, the reads were annotated to the Genome Reference Consortium Mouse Build 39 (mm39) using the STAR method. Quantification was conducted using RefSeq release 93. Differential expression analysis was performed using the R package DESeq2. Genes showing an absolute 1.5-fold-change and FDR <0.05 were used as DEGs. DEGs were subjected to ingenuity pathway analysis using ingenuity pathway analysis (IPA) software (www.ingenuity.com). The statistical significance of the enrichment of specific pathways among the DEGs was investigated using Fisher's exact test. Our RNA-seq data have been submitted to the Gene Expression Omnibus (accession number GSE216063).

Protein extraction and western blotting

Hypothalamus isolated from mice was transferred to 300μl Tissue Extraction Reagent 1 (Cat# FNN0071; Invitrogen) with 3μl protease inhibitor (Cat# P-2714; Sigma-Aldrich, St. Louis, MO, USA) and homogenized. Pierce BCA Protein Assay Kit (Cat# 23227; Thermo Fisher Scientific) was used to determine the conentration of protein samples. Each protein lysate (20μg) was run on sodium dodecyl sulfate polyacrylamide gel electrophoresis gel, transferred to a polyvinylidene fluoride membrane, blocked for 1 h at 24 °C with 5% fat-free milk in Tris-buffered saline containing 0.1% Tween 20, and incubated with monoclonal rabbit anti-CREB (1:500) (Cat# ab32515; Abcam, Cambridge, UK; RRID:AB_2292301), rabbit and anti-phospho-CREB (1:1,000) (Cat# 9198S; Cell Signaling Technology, Danvers, MA, USA; RRID:AB_2561044). Mouse anti-α-tubulin (1:10,000) (Cat# T5168, Sigma-Aldrich, St. Louis, MO, USA; RRID:AB_477579) was used as a control. Horseradish peroxidase-conjugated goat anti-rabbit secondary antibodies (1:5,000) (Cat# 7074S; Cell Signaling Technology,

Song *et al. BMC Biology*   (2023) 21:243

Page 11 of 14

Danvers, MA, USA; RRID:AB_2099233) and goat anti-mouse secondary antibodies (1:10,000) (Cat# G21040; Invitrogen, Carlsbad, CA, USA; RRID:AB_2536527) were used for detection. Enhanced chemiluminescence western blot detection reagents (Amersham Pharmacia Biotech, Piscataway, NJ, USA) were used to detect the target proteins. $n = 3$ mice/group.

Enzyme-linked immunosorbent assay
BDNF protein expression was quantified using a duo-set ELISA assay (Cat# DY248, R&D systems, Minneapolis, MN, USA) according to the manufacture's instructions. Briefly, standards and samples diluted with assay buffer were incubated with detection antibody for 2 hrs at room temperature. TMB was used as the substrate to detect the bound detection antibodies. Optical density was measured at 450nm. $n = 4$ mice/group.

Nissl staining
After the 12th week of diet consumption, transcardial perfusion of the mice was performed with 4% paraformaldehyde for 14-16h fixation. The tissues were processed and embedded in paraffin. A rotary microtome was used to section the hypothalamus. The 4 μm-thick hypothalamic coronal sections were deparaffinized and hydrated using distilled water. Cresyl violet acetate (1.0% aqueous) was applied to the tissue for 5 min and then quickly rinsed in 1 mL of distilled water. After quick dehydration in absolute alcohol, the tissues were cleared in xylene and mounted in synthetic resin. Motic Digital Slide Assistant software v1.0.7.61b (Motic China Group Co., Ltd, NY, USA) was used to analyze the histology of the samples. To count Nissl-stained cells in the hypothalamus, ImageJ software v1.53e (National Institutes of Health, Bethesda, MD, USA) was used. $n = 4$ slices from 2 mice/group.

Immunohistochemistry
Hypothalamus sections of 4 μm thickness were prepared from paraffin-embedded specimens. To identify newborn neurons (DCX+), we conducted dewaxing, antigen retrieval, antibody incubation, staining, and sealing. DCX antigen was retrieved using sodium citrate (pH 6·0). Sections were incubated 14-16h at 4 °C with the primary antibody anti-DCX (1:200; Cat# ab18723; Abcam). The sections were then incubated with goat anti-rabbit IgG (Cat# A16101, ThermoFisher Scientific, USA). Immunoreactive cells were visualized and captured using a fluorescence microscope (BX53, Olympus, Tokyo, Japan) and digital camera (INFINITY3, Lumenera, Ottawa, Canada) at 200 × magnification. ImageJ software v1.53e (National Institutes of Health, Bethesda, MD, USA) was used for analysis. $n = 2$ slices from 2 mice/group.

Cell culture
mHypoA-2/12 cells (Cat # CLU177; Cellutions Biosystem Inc., Toronto, Canada) were cultured in $1 \times$ Dulbecco's modified Eagle's medium (Cat # LM001-07; WelGENE Inc., Daegu, Korea) supplemented with 10% fetal bovine serum and 1% penicillin/streptomycin at 37 °C with 5% CO_2.

In vitro knockdown with siRNA
For the knockdown of *Tas1r3*, 3×10^4 mHypoA-2/12 cells per well were seeded in a 6-well culture plate approximately 24 hr prior to transfection. After the cells had grown to 50–60% confluency, 40nM of *Tas1r3* siRNA (Bioneer, Daejeon, Korea) and negative control siRNA (Bioneer) complexed with Lipofectamine RNAiMAX® (Invitrogen, ThermoFisher Scientific, USA) were added to each well according to the manufacturer's instructions and incubated for 48 hr at 37 °C. On the day of the experiments, the transfection medium was removed, and the supernatants were replaced with no glucose medium (Cat # LM001-06, WelGENE) or medium containing 10mM glucose, 10mM fructose and 10μM palmitate. The cells were then incubated for 0, 12, and 24 hr at 37 °C. Following incubation, cell viability at each time point was measured using Countess™ 3 Automated Cell Counters (Invitrogen). Then, the cells were washed with phosphate buffered saline, and RNA was isolated for qPCR. The target sequences of the siRNA are listed in Additional file 2: Table S2.

Quantitative real-time PCR (qPCR)
Reverse transcription and real-time PCR were conducted as previously described [63]. The primers used for qPCR are listed in Additional file 2: Table S3. $n = 3$/group.

Statistical analyses
Two-way ANOVA was used for the statistical analysis of multiple experimental groups with a Tukey's post-hoc test. Analysis of anxiety-related parameters with body weight as the covariate was performed using ANCOVA. An unpaired two-tailed Student's *t*-test was used to compare two groups. Differences were considered significant when the *p*-value was < 0.05. All data are presented as mean ± SEM. In gene expression profiling, a right-tailed Fisher's exact test was used to determine the significant biological pathways enriched with DEGs. GraphPad Prism version 9.00 for Windows (GraphPad, Inc., San Diego, CA, USA), IBM SPSS Statistics v25 (IBM Corp., Armonk, NY, USA), Partek Flow software (Partek, St. Louis, MO, USA; http://www.partek.com/partekgs), and IPA were used for the statistical analyses.

Song *et al. BMC Biology*   (2023) 21:243

Page 12 of 14

Abbreviations

ANCOVA	One-way analysis of covariance
ANOVA	Analysis of variance
BDNF	Brain-derived neurotrophic factor
CREB	CAMP response element binding protein
DEGs	Differentially expressed genes
ELISA	Enzyme-linked immunosorbent assay
EPM	Elevated plus maze
FDR	False discovery rate
GSEA	Gene set enrichment analysis
IPA	Ingenuity pathway analysis
LDB	Light–dark box
ND	Normal diet
NSF	Novelty-suppressed feeding
OF	Open field
PKA	Protein kinase A
TAS1R3	Taste receptor type 1 member 3
WD	Western diet
WT	Wild-type

Supplementary Information

The online version contains supplementary material available at https://doi.org/10.1186/s12915-023-01723-x.

Additional file 1: Fig. S1. Caloric intake of male WT and *Tas1r3*$^{-/-}$ mice fed ND or WD for 12 weeks. **Fig. S2.** Correlation graphs between body weight and anxiety-related parameters. **Fig. S3.** Body weight, locomotor activities and anxiety-related behaviors of female WT and *Tas1r3*$^{-/-}$ mice fed ND or WD for 12 weeks. **Fig. S4.** Representative images and quantitative analysis of Nissl staining of hypothalamus. **Fig. S5.** *Tas1r3*, *Prkaca*, *Creb1* and *Bdnf* mRNA expression in the hippocampal tissue and cultured adult hippocampal neuronal cell line.

Additional file 2: Table S1. Cohorts of animals used for behavioral testing. **Table S2.** siRNA target sequences. **Table S3.** qPCR primers.

Additional file 3: Raw Data. Raw data underlying Fig. 1, Figs. 3-5, and Fig. S5.

Additional file 4: Fig. S6. Uncropped western blot figures.

Acknowledgements
Not applicable.

Authors' contributions
Conceptualization, W.S. and D.S.; investigation, J.W.S., K.L. H.S. and W.S.; methodology, J.W.S., W.S. and D.S.; writing-original draft, J.W.S. and W.S.; funding acquisition, W.S. and D.S.; supervision, W.S. and D.S. All authors read and approved the final manuscript.

Availability of data and materials
All data generated or analysed during this study are included in this published article, its supplementary information files and publicly available repositories. The raw transcriptome datasets generated during the current study are available in the Gene Expression Omnibus database (available online: http://www.ncbi.nlm.nih.gov/geo) (accession numbers GSE216063) The data that support the findings of this study are available from the corresponding author upon reasonable request. The individual data values for Figs. 1, 3, 4, and 5, as well as Additional file 1: Fig. S5, are provided in Additional file 3.

Declarations

Ethics approval and consent to participate
All protocols involving rodents were approved by the Institutional Animal Care and Use Committee of Seoul National University (approval number: SNU-181001-2; Seoul, Korea).

Consent for publication
Not applicable.

Competing interests
The authors declare that they have no competing interests.

References

1. Association AP. American Psychiatric Association: Diagnostic and Statistical Manual of Mental Disorders, Arlington. 2013
2. Collaborators GMD. Global, regional, and national burden of 12 mental disorders in 204 countries and territories, 1990–2019: a systematic analysis for the Global Burden of Disease Study 2019. Lancet Psychiatry. 2022;9(2):137–50.
3. Yang X, Fang Y, Chen H, Zhang T, Yin X, Man J, et al. Global, regional and national burden of anxiety disorders from 1990 to 2019: results from the Global Burden of Disease Study 2019. Epidemiol Psychiatr Sci. 2021;30:36. https://doi.org/10.1017/s2045796021000275.
4. Afifi TO, Mota NP, Dasiewicz P, MacMillan HL, Sareen J. Physical punishment and mental disorders: results from a nationally representative US sample. Pediatrics. 2012;130(2):184–92.
5. Moylan S, Jacka FN, Pasco JA, Berk M. Cigarette smoking, nicotine dependence and anxiety disorders: a systematic review of population-based, epidemiological studies. BMC Med. 2012;10(1):1–14.
6. Mwinyi J, Pisanu C, Castelao E, Stringhini S, Preisig M, Schiöth HB. Anxiety disorders are associated with low socioeconomic status in women but not in men. Womens Health Issues. 2017;27(3):302–7.
7. Rangel C, Dukeshire S, MacDonald L. Diet and anxiety. An exploration into the Orthorexic Society. Appetite. 2012;58(1):124–32.
8. Aucoin M, LaChance L, Naidoo U, Remy D, Shekdar T, Sayar N, et al. Diet and anxiety: a scoping review. Nutrients. 2021;13(12):4418.
9. Popkin BM, Adair LS, Ng SW. Global nutrition transition and the pandemic of obesity in developing countries. Nutr Rev. 2012;70(1):3–21. https://doi.org/10.1111/j.1753-4887.2011.00456.x.
10. Canetti L, Bachar E, Bonne O. Deterioration of mental health in bariatric surgery after 10 years despite successful weight loss. Eur J Clin Nutr. 2016;70(1):17–22.
11. Ogrodnik M, Zhu Y, Langhi LGP, Tchkonia T, Krüger P, Fielder E, et al. Obesity-induced cellular senescence drives anxiety and impairs neurogenesis. Cell Metab. 2019;29(5):1061-77.e8. https://doi.org/10.1016/j.cmet.2018.12.008.
12. Price JL, Drevets WC. Neurocircuitry of mood disorders. Neuropsychopharmacology. 2010;35(1):192–216. https://doi.org/10.1038/npp.2009.104.
13. Schaeffer M, Langlet F, Lafont C, Molino F, Hodson DJ, Roux T, et al. Rapid sensing of circulating ghrelin by hypothalamic appetite-modifying neurons. Proc Natl Acad Sci U S A. 2013;110(4):1512–7. https://doi.org/10.1073/pnas.1212137110.
14. Lam TKT, Schwartz GJ, Rossetti L. Hypothalamic sensing of fatty acids. Nat Neurosci. 2005;8(5):579–84. https://doi.org/10.1038/nn1456.
15. Lama A, Pirozzi C, Severi I, Morgese MG, Senzacqua M, Annunziata C, et al. Palmitoylethanolamide dampens neuroinflammation and anxiety-like behavior in obese mice. Brain Behav Immun. 2022;102:110–23.
16. Hillman JB, Dorn LD, Loucks TL, Berga SL. Obesity and the hypothalamic-pituitary-adrenal axis in adolescent girls. Metabolism. 2012;61(3):341–8.
17. Recabal A, Caprile T, García-Robles MLA. Hypothalamic neurogenesis as an adaptive metabolic mechanism. Front Neurosci. 2017;11:190. https://doi.org/10.3389/fnins.2017.00190.

Song *et al. BMC Biology*   (2023) 21:243

Page 13 of 14

18. Samodien E, Chellan N. Hypothalamic neurogenesis and its implications for obesity-induced anxiety disorders. Front Neuroendocrinol. 2021;60:100871. https://doi.org/10.1016/j.yfrne.2020.100871.

19. Sanematsu K, Yoshida R, Shigemura N, Ninomiya Y. Structure, function, and signaling of taste G-protein-coupled receptors. Curr Pharm Biotechnol. 2014;15(10):951–61. https://doi.org/10.2174/13892010156661409221 05911.

20. Zhao GQ, Zhang Y, Hoon MA, Chandrashekar J, Erlenbach I, Ryba NJ, et al. The receptors for mammalian sweet and umami taste. Cell. 2003;115(3):255–66. https://doi.org/10.1016/s0092-8674(03)00844-4.

21. Gong T, Wang W, Xu H, Yang Y, Chen X, Meng L, et al. Longitudinal expression of testicular TAS1R3 from Prepuberty to sexual maturity in Congjiang Xiang pigs. Animals (Basel). 2021;11(2). https://doi.org/10. 3390/ani11020437.

22. Harrington EO, Vang A, Braza J, Shil A, Chichger H. Activation of the sweet taste receptor, T1R3, by the artificial sweetener sucralose regulates the pulmonary endothelium. Am J Physiol Lung Cell Mol Physiol. 2018;314(1):L165–76. https://doi.org/10.1152/ajplung.00490.2016.

23. Dyer J, Salmon KS, Zibrik L, Shirazi-Beechey SP. Expression of sweet taste receptors of the T1R family in the intestinal tract and enteroendocrine cells. Biochem Soc Trans. 2005;33(Pt 1):302–5. https://doi.org/10. 1042/bst0330302.

24. Ren X, Zhou L, Terwilliger R, Newton SS, de Araujo IE. Sweet taste signaling functions as a hypothalamic glucose sensor. Front Integr Neurosci. 2009;3:12. https://doi.org/10.3389/neuro.07.012.2009.

25. Elizondo-Vega RJ, Recabal A, Oyarce K. Nutrient Sensing by Hypothalamic Tanycytes. Front Endocrinol (Lausanne). 2019;10:244. https://doi. org/10.3389/fendo.2019.00244.

26. Swanson L, Sawchenko P. Paraventricular nucleus: a site for the integration of neuroendocrine and autonomic mechanisms. Neuroendocrinology. 1980;31(6):410–7.

27. Vagena E, Ryu JK, Baeza-Raja B, Walsh NM, Syme C, Day JP, et al. A high-fat diet promotes depression-like behavior in mice by suppressing hypothalamic PKA signaling. Transl Psychiatry. 2019;9(1):141. https:// doi.org/10.1038/s41398-019-0470-1.

28. Auguste S, Fisette A, Fernandes MF, Hryhorczuk C, Poitout V, Alquier T, et al. Central agonism of GPR120 acutely inhibits food intake and food reward and chronically suppresses anxiety-like behavior in mice. Int J Neuropsychopharmacol. 2016;19(7):pyw014.

29. Zhao G, Ford ES, Dhingra S, Li C, Strine TW, Mokdad A. Depression and anxiety among US adults: associations with body mass index. Int J Obes. 2009;33(2):257–66.

30. Tang F, Wang G, Lian Y. Association between anxiety and metabolic syndrome: A systematic review and meta-analysis of epidemiological studies. Psychoneuroendocrinology. 2017;77:112–21.

31. Bangasser DA, Cuarenta A. Sex differences in anxiety and depression: circuits and mechanisms. Nat Rev Neurosci. 2021;22(11):674–84.

32. Finkbeiner S, Tavazoie SF, Maloratsky A, Jacobs KM, Harris KM, Greenberg ME. CREB: a major mediator of neuronal neurotrophin responses. Neuron. 1997;19(5):1031–47. https://doi.org/10.1016/s0896-6273(00) 80395-5.

33. Souza C, Moreira J, Siqueira I, Pereira A, Rieger D, Souza D, et al. Highly palatable diet consumption increases protein oxidation in rat frontal cortex and anxiety-like behavior. Life Sci. 2007;81(3):198–203.

34. Hunsche C, de Toda IM, De la Fuente M. Impacts of the late adulthood diet-induced obesity onset on behavior, immune function, redox state and life span of male and female mice. Brain Behav Immun. 2019;78:65–77.

35. Clark TD, Crean AJ, Senior AM. Obesogenic diets induce anxiety in rodents: A systematic review and meta-analysis. Obes Rev. 2022;23(3):e13399.

36. Fulton S, Décarie-Spain L, Fioramonti X, Guiard B, Nakajima S. The menace of obesity to depression and anxiety prevalence. Trends Endocrinol Metab. 2022;33(1):18–35. https://doi.org/10.1016/j.tem.2021.10.005.

37. Simon BR, Learman BS, Parlee SD, Scheller EL, Mori H, Cawthorn WP, et al. Sweet taste receptor deficient mice have decreased adiposity and increased bone mass. PLoS ONE. 2014;9(1):e86454. https://doi.org/10. 1371/journal.pone.0086454.

38. Murovets VO, Sozontov EA, Zachepilo TG. The effect of the taste receptor protein T1R3 on the development of islet tissue of the murine pancreas. Dokl Biol Sci. 2019;484(1):1–4. https://doi.org/10.1134/s0012 496619010010.

39. Glendinning JI, Gillman J, Zamer H, Margolskee RF, Sclafani A. The role of T1r3 and Trpm5 in carbohydrate-induced obesity in mice. Physiol Behav. 2012;107(1):50–8. https://doi.org/10.1016/j.physbeh.2012.05. 023.

40. Murovets VO, Bachmanov AA, Zolotarev VA. Impaired Glucose Metabolism in Mice Lacking the Tas1r3 Taste Receptor Gene. PLoS ONE. 2015;10(6):e0130997. https://doi.org/10.1371/journal.pone.0130997.

41. Martin B, Wang R, Cong WN, Daimon CM, Wu WW, Ni B, et al. Altered learning, memory, and social behavior in type 1 taste receptor subunit 3 knock-out mice are associated with neuronal dysfunction. J Biol Chem. 2017;292(27):11508–30. https://doi.org/10.1074/jbc.M116. 773820.

42. Blouet C, Schwartz GJ. Hypothalamic nutrient sensing in the control of energy homeostasis. Behav Brain Res. 2010;209(1):1–12. https://doi. org/10.1016/j.bbr.2009.12.024.

43. Yang L, McKnight GS. Hypothalamic PKA regulates leptin sensitivity and adiposity. Nat Commun. 2015;6:8237. https://doi.org/10.1038/ ncomms9237.

44. Molteni R, Barnard RJ, Ying Z, Roberts CK, Gómez-Pinilla F. A high-fat, refined sugar diet reduces hippocampal brain-derived neurotrophic factor, neuronal plasticity, and learning. Neuroscience. 2002;112(4):803–14. https://doi.org/10.1016/s0306-4522(02)00123-9.

45. Wang CS, Kavalali ET, Monteggia LM. BDNF signaling in context: From synaptic regulation to psychiatric disorders. Cell. 2022;185(1):62–76. https://doi.org/10.1016/j.cell.2021.12.003.

46. Sakamoto K, Karelina K, Obrietan K. CREB: a multifaceted regulator of neuronal plasticity and protection. J Neurochem. 2011;116(1):1–9. https://doi.org/10.1111/j.1471-4159.2010.07080.x.

47. Wand G. The anxious amygdala: CREB signaling and predisposition to anxiety and alcoholism. J Clin Invest. 2005;115(10):2697–9. https://doi. org/10.1172/jci26436.

48. Suliman S, Hemmings SM, Seedat S. Brain-Derived Neurotrophic Factor (BDNF) protein levels in anxiety disorders: systematic review and meta-regression analysis. Front Integr Neurosci. 2013;7:55.

49. McMurphy T, Huang W, Liu X, Siu JJ, Queen NJ, Xiao R, et al. Hypothalamic gene transfer of BDNF promotes healthy aging in mice. Aging Cell. 2019;18(2):e12846. https://doi.org/10.1111/acel.12846.

50. Martinowich K, Manji H, Lu B. New insights into BDNF function in depression and anxiety. Nat Neurosci. 2007;10(9):1089–93. https://doi. org/10.1038/nn1971.

51. Engel DF, Bobbo VCD, Solon CS, Nogueira GA, Moura-Assis A, Mendes NF, et al. Activation of GPR40 induces hypothalamic neurogenesis through p38- and BDNF-dependent mechanisms. Sci Rep. 2020;10(1):11047. https://doi.org/10.1038/s41598-020-68110-2.

52. Petrik D, Encinas JM. Perspective: of mice and men–how widespread is adult neurogenesis? Front Neurosci. 2019;13:923.

53. Batailler M, Droguerre M, Baroncini M, Fontaine C, Prevot V, Migaud M. DCX-expressing cells in the vicinity of the hypothalamic neurogenic niche: a comparative study between mouse, sheep, and human tissues. J Compar Neurol. 2014;522(8):1966–85.

54. McNay DE, Briançon N, Kokoeva MV, Maratos-Flier E, Flier JS. Remodeling of the arcuate nucleus energy-balance circuit is inhibited in obese mice. J Clin Investig. 2012;122(1):142–52.

55. Nascimento LF, Souza GF, Morari J, Barbosa GO, Solon C, Moura RF, et al. n-3 fatty acids induce neurogenesis of predominantly POMC-expressing cells in the hypothalamus. Diabetes. 2016;65(3):673–86. https://doi. org/10.2337/db15-0008.

56. Xie Y, Kaufmann D, Moulton MJ, Panahi S, Gaynes JA, Watters HN, et al. Lef1-dependent hypothalamic neurogenesis inhibits anxiety. PLoS Biol. 2017;15(8):e2002257. https://doi.org/10.1371/journal.pbio.2002257.

57. Sousa-Ferreira L, Álvaro AR, Aveleira C, Santana M, Brandão I, Kügler S, et al. Proliferative hypothalamic neurospheres express NPY, AGRP, POMC, CART and Orexin-A and differentiate to functional neurons. PLoS ONE. 2011;6(5):e19745. https://doi.org/10.1371/journal.pone. 0019745.

58. Li C, Hou Y, Zhang J, Sui G, Du X, Licinio J, et al. AGRP neurons modulate fasting-induced anxiolytic effects. Transl Psychiatry. 2019;9(1):111. https://doi.org/10.1038/s41398-019-0438-1.

59. Dixon CI, Rosahl TW, Stephens DN. Targeted deletion of the GABRA2 gene encoding alpha2-subunits of GABA(A) receptors facilitates performance of a conditioned emotional response, and abolishes anxiolytic effects of benzodiazepines and barbiturates. Pharmacol Biochem Behav. 2008;90(1):1–8. https://doi.org/10.1016/j.pbb.2008.01.015.

60. Enoch MA, Schwartz L, Albaugh B, Virkkunen M, Goldman D. Dimensional anxiety mediates linkage of GABRA2 haplotypes with alcoholism. Am J Med Genet B Neuropsychiatr Genet. 2006;141b(6):599–607. https://doi.org/10.1002/ajmg.b.30336.

61. Sriram K, Insel PA. G protein-coupled receptors as targets for approved drugs: how many targets and how many drugs? Mol Pharmacol. 2018;93(4):251–8. https://doi.org/10.1124/mol.117.111062.

62. Shon W-J, Lee Y-K, Shin JH, Choi EY, Shin D-M. Severity of DSS-induced colitis is reduced in Ido1-deficient mice with down-regulation of TLR-MyD88-NF-kB transcriptional networks. Sci Rep. 2015;5(1):17305. https://doi.org/10.1038/srep17305.

63. Shon WJ, Park MN, Lee J, Shin JH, Shin DM. Renal transcriptome profiles in mice reveal the need for sufficient water intake irrespective of the drinking water type. Sci Rep. 2022;12(1):10911. https://doi.org/10.1038/s41598-022-14815-5.

Publisher's Note